JOURNAL OF NANO- AND ELECTRONIC PHYSICS
Vol. **5** No 2, 02024(3pp) (2013)

ЖУРНАЛ НАНО- ТА ЕЛЕКТРОННОЇ ФІЗИКИ
Том **5** № 2, 02024(3cc) (2013)

Pulsed Laser Deposited Nickel Doped Zinc Oxide Thin Films: Structural and Optical Investigations

Tanveer A. Dar*, Arpana Agrawal, Pratima Sen

Laser Bhawan, School of Physics, Devi Ahilya University, Takshashila Campus, Indore-452001, India

(Received 15 February 2013; revised manuscript received 28 April 2013; published online 04 May 2013)

Structural and optical studies has been done on Nickel doped Zinc Oxide ($Ni_xZn_{1-x}O$, x = 0.03, 0.05 and 0.07 by weight) thin films prepared by pulsed laser deposition technique. The films are characterized by X-ray diffraction, Uv-vis spectroscopy, X-ray photoelectron spectroscopy. We observed a slight red shift in the optical band gap in the NiZnO subsequent to Ni doping. This shift can be assigned due to the sp-d exchange interaction of Ni- d states with s and p-states of ZnO. Also X-ray photoelectron spectroscopy studies show that Ni has well substituted in + 2 oxidation state by replacing Zn^{2+}.

Keywords: Semiconductors, II–VI semiconductors, Doping, Exchange interactions.

PACS numbers: 68.55.ag, 73.61.Ga, 79.60.Dp 71.70.Gm

1. INTRODUCTION

The phenomenon of band gap engineering and integration of magnetic properties in semiconductor materials is currently an active field of research. These modifications have been found to provide a huge interest in high technological applications like light emitting diodes [1], lasers [2] and also in spin transport media. One of the host materials for such potential applications is a II-VI wide band gap semiconductor namely Zinc Oxide (ZnO) which has been extensively studied with proper impurity doping. Due to the ability of absorbing ultra-voilet light because of large and wide band gap, ZnO has found huge applications in sunscreens and also in varistors and pigments.

Electrically ZnO is an *n*-type degenerate semiconductor with huge dielectric constant and exhibits activated conduction behaviour [3]. ZnO possess hexagonal wurtzite structure where there is a tetrahedral coordination of Zn atoms with four oxygen atoms. The Zn *s* - electrons hybridize with the oxygen *p*-electrons. Introducing impurities by an appropriate method in ZnO not only provides an insight into the study of its electronic properties, but also provides a great interest in studying its optical properties. The isovalent nature of ZnO and transition metal ions (TMIs) has made it possible to dope ZnO with Al [4], Ga [5-7], Co, Ni [8], Cd [9] and Mg [10]. There has been a great deal of attention on search for magnetism in transition metal (TM) ion doped ZnO [11-16] which will make it an important candidate for dilute magnetic Semiconductor (DMS) spintronic applications.

Ni doped ZnO has been observed as an important candidate in the field of DMSs [8]. A very few studies has been carried out on NiZnO system due to the phase segregation of ZnO and NiO. This happens due the large driving force of Ni-O bond as compared to Zn-O bond [17].

2. EXPERIMENTAL DETAILS

Pure ZnO and $Ni_xZn_{1-x}O$ (x = 0.03, 0.05, 0.07 by weight) bulk targets were prepared by standard solid state reaction methods. The targets were calcinated at 900 °C followed by sintering at 1400 °C for about 36 hours. The targets were finally made in the form of 25 mm diameter pellets. Thin films from the prepared pellets were deposited on glass substrate by pulsed laser deposition technique (PLD) using an excimer (KrF) laser at 248 nm wavelength to ablate the target. The pulse duration of the laser was 20 ns with repetition rate of 10 Hz and the energy density was 2 J/cm^2. Deposition was carried out in a vacuum chamber pumped down to a base pressure of 4 nbar and oxygen gas was flown into the chamber at 1 nbar. The target-to-substrate distance was maintained at 5 cm with optimized substrate temperature of 400 °C. X-ray photoelectron spectroscopy (XPS) measurements were performed at Angle Integrated Photo-electron Beamline on INDUS-1 Synchrotron radiation source at RRCAT, Indore. To reduce the contamination effect, all the samples were subjected to a surface clean procedure by Ar^+ bombardment in the vacuum chamber equipped in the XPS instrument.

3. RESULTS AND DISCUSSION

3.1 X-ray Diffraction (XRD)

The XRD data were obtained from the D8 advanced Bruker XRD machine using CuKα source. The XRD patterns of $Ni_xZn_{1-x}O$ films at different concentrations of nickel (0 %, 3 %, 7 % by weight) are shown in Fig. 1. The mean grain size of the thin film samples were calculated using the Scherrer equation to the (002) plane diffraction peak. The mean Scherer grain sizes of pure and Ni-doped ZnO thin films are 40.74, 26.12, 24.35 and 30.32 nm, respectively. The results reveal that Ni doped ZnO thin films can reduce the average crystallite size for the 3 and 5 % samples, however the grain size of 7 % doped sample increases due to strain relaxation process in the film. The strain relaxation appears due to the phase segregation of NiO and increasing doping concentration of Ni in ZnO matrix [18]. The c-axis

* tanveerphysics@gmail.com

lattice parameter of the samples is calculated from the reflection (002) peak using the formula:

$$c = \lambda / \sin\theta$$

where θ is the diffraction angle corresponding to (002) plane, λ is incident wavelength ($\lambda = 0.15406$ nm).

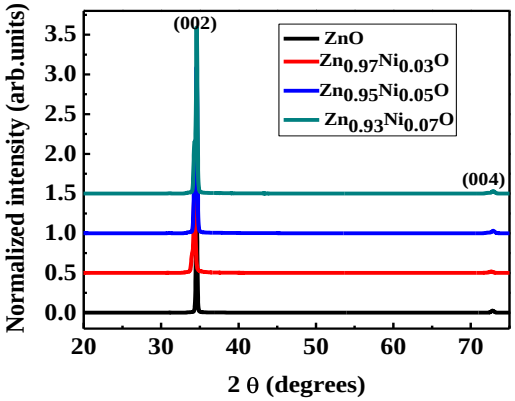

Fig. 1 – XRD Patterns of Ni doped ZnO thin films on glass substrate

The obtained results show the dimensions of **c** in doped and undoped samples as 5.180, 5.221, 5.219 and 5.188 Å for ZnO and NiZnO (Ni = 3, 5 and 7 %) thin films, respectively. The variation of lattice constant c is due to the difference in the ionic radii of Zn^{2+} and Ni^{2+}. Change in lattice constant is related to oxygen deficiency and or existence of Ni^{3+}.

3.2 Uv-Vis Spectroscopy

Typical room temperature optical absorption spectra for $Ni_xZn_{1-x}O$ samples ($x = 0$, 3, 5 and 7 %) are shown in Fig. 2. The band gap energies of the samples were determined by taking the intersection of the extrapolated lines from the linear vertical regions near the band edge.

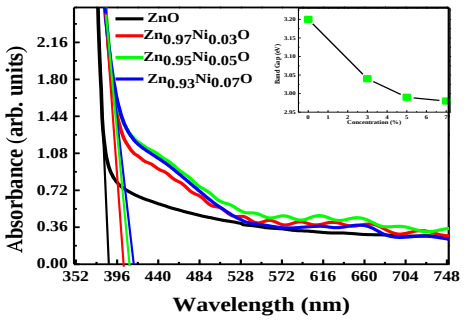

Fig. 2 – Absorption edges of the films with increasing Ni concentration and the inset shows variation of the band edge with x

ZnO being a direct band gap semiconductor has an absorption coefficient, which obeys the following relation for high-photon energies:

$$\alpha h\upsilon = A(h\upsilon - E_g)^{1/2},$$

where A is a constant, α the absorption coefficient (cm^{-1}) and $h\upsilon$ (eV) is the energy of excitation. The absorbance is expected to depend on several factors, such as band gap, oxygen deficiency surface roughness and impurity centers [19]. The measured direct band gap energy of the ZnO films with different Ni concentrations at 3, 5, and 7 % were, 3.06, 2.99 and 2.98 eV, respectively. The band gap value for pure ZnO was found to be 3.23 eV.

The absorption edges of the films with increasing Ni concentration shows red shift i.e. decrease in the band gap. The optical absorption at absorption edge corresponds to the transition from valence band to conduction band, while the absorption edge shifting to the lower energy relates to some local energy levels caused by some intrinsic defects [20]. The possible reason for decrease in band gap is put as follows: the impurity states of d-electrons of Ni split under the influence of tetrahedral field of ZnO giving rise to lower energy e_g doublet and higher energy t_{2g} triplet states. The triplet states hybridize with valence p-states forming $t_{\{bonding\}}$ and $t_{\{antibonding\}}$ states. These states lie within the band gap such that bonding states are near the valence band and antibonding states occur near the conduction band edge [21]. The optical absorption takes place among these states and manifests in the red shift of the cut-off wavelength, reducing the band gap.

3.3 XPS Results

To confirm the valence state of the Ni element and the modifications in the electronic structure of $Ni_xZn_{1-x}O$, subsequent to Ni doping in ZnO in the ZnO lattice, XPS measurement is performed. The binding energies were corrected for the charging effect with reference to the C 1 s line at 284.6 eV. The Experiment was performed at Angle Integrated photo-electron Beamline on INDUS-1 Synchrotron radiation source RRCAT Indore. The Ni $2p_{3/2}$ peak for $Zn_{1-x}Ni_xO$ ($x = 0.03$, 0.05, 0.07 by weight) occurs at around ~ 853 eV while as Ni $2p_{3/2}$ occurs at around ~ 873 eVs. Corresponding satellite structures were clearly observed around 861 eV and 879 eV, respectively. The peak positions depend on the local structure of the Ni atoms, providing information on the chemical state.

The Ni $2p_{3/2}$ peak position is quite different from that of NiO, while close to the value of Ni. The energy difference between Ni $2p_{3/2}$ and $2p_{1/2}$ peaks in Zn_xNi_{1-x} ($x = 03{,}05$ and 0.07 by composition) is 16.893 eV, 16.812 eV, and 17.44 eV respectively, which strikingly differs from 18.4 eV of NiO [22], indicating that Ni substituted for the Zn site of the lattice instead of forming the second phase of NiO. So we can conclude that Ni has been incorporated in ZnO matrix and no other phase of NiO is formed which is further confirmed by XRD results above.

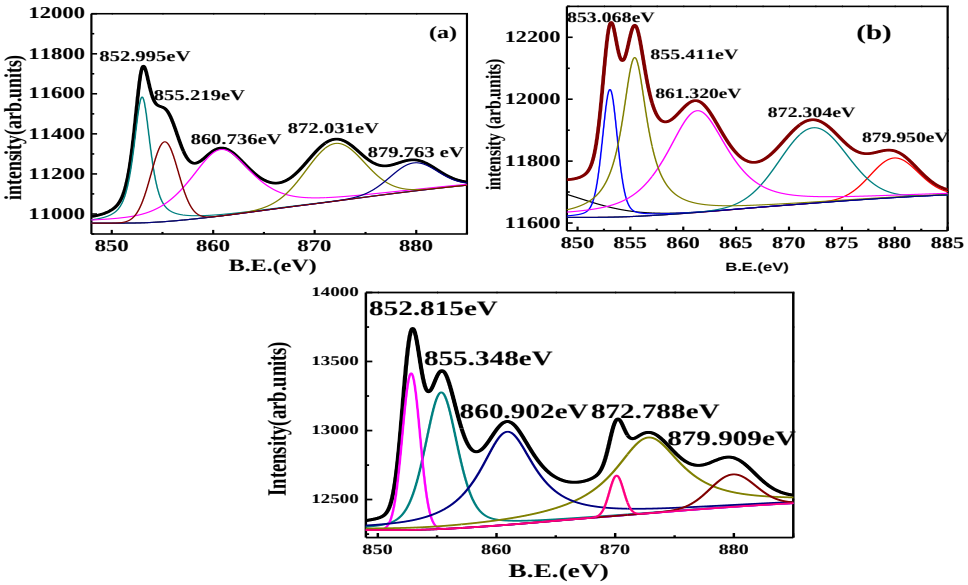

Fig. 3 – XPS core level spectrum of Ni $2p_{3/2}$ in (a) $Zn_{0.97}Ni_{0.07}O$, (b) $Zn_{0.95}Ni_{0.05}O$, (c) $Zn_{0.93}Ni_{0.07}O$, respectively

4. CONCLUSION

Polycrystalline Ni doped ZnO films has been prepared by PLD technique. No impurity phases have been observed from structural analysis. The red shift in the band gap is observed. This property along with the magnetic nature of NiZnO can be used for magneto optic effects. Ni doping in ZnO makes the alloy semiconductor a potential Diluted Magnetic Semiconductor (DMS).

ACKNOWLEDGEMENTS

Authors are grateful to UGC-DAE CSR Indore for providing characterisation facilities, and financial support. We also thank Dr. Pankaj Misra, RRCAT, Indore for providing experimental facilities during sample preparation.

REFERENCE

1. J. Singh, *Semiconductor Optoelectronics:* (Physics and Technology) (New York: McGraw Hill: 1995).
2. A.H. Herzog, D.L. Keune, M.G. Craford, *J. Appl. Phys.* **43**, 600 (1972).
3. S. Singh, N. Rama, K. Sethupathi, M.S.R. Rao, *J. Appl. Phys.* **103**, 07D108 (2008).
4. A. Segura, J.A. Sans, D. Errandonea, D. Martinez-García, V. Fages, *Appl. Phys. Lett.* **88**, 011910 (2006).
5. T. Makino, Y. Segawa, S. Yoshida, A. Tsukazaki, A. Ohtomo, M. Kawasaki, *Appl. Phys. Lett.* **85**, 759 (2004).
6. J. Zhong, S. Muthukumar, Y. Chen, Y. Lu, H.M. Ng, W. Jiang, E.L. Garfunkel, *Appl. Phys. Lett.* **83**, 3401 (2003).
7. C. Xu, M. Kim, J. Chun, D. Kim, *Appl. Phys. Lett.* **86**, 133107 (2005).
8. J.B. Cui, U.J. Gibson, *Appl. Phys. Lett.* **87**, 133108 (2005).
9. Q.H. Li, Q. Wan, Y.G. Wang, T.H. Wang, *Appl. Phys. Lett.* **86**, 263101 (2005).
10. C. Xu, M. Kim, J. Chun, D. Kim, *Appl. Phys. Lett.* **86**, 133107 (2005).
11. K. Sato, H. Katayama-Yoshida, *Physica B* **308–310**, 904 (2001).
12. K. Ueda, H. Tabota, T. Kamai, *Appl. Phys. Lett.* **79**, 988 (2000).
13. N.H. Hong, J. Sakai, A. Hassini, *J. Phys: Condens. Mat.* **17**, 199 (2005).
14. T. Wakano, N. Fujimura, Y. Morinaga, N. Abe, A. Ashida, T. Ito, *Physica E* **10**, 260 (2001).
15. W. Jung, S.J. An, G.C. Yi, C.U. Jung, S.I. Lee, S. Cho, *Appl. Phys. Lett.* **80**, 4561 (2002).
16. B. Srinivasa Rao, B. Rajesh Kumar, G. Venkata Chalapathi, V. Rajagopal Reddy, T. Subba Rao, *J. Nano- Electron. Phys.* **3**, No 1, 620 (2011).
17. J. Mohapatra, D.K. Mishra, S.K. Kamilla, V.R.R. Medicherla, D.M. Phase, V. Berma, S.K. Singh, *phys. status solidi b* **248**, 1352 (2011).
18. A.S. Ahmed, S.M. Muhamed, M.L. Singla, S. Tabassum, A.H. Naqvi, A. Azam. *J. Lumin.* **131**, 1 (2011).
19. W. Yu, L.H. Yang, X.Y. Teng, J.C. Zhang, Z.C. Zhang. L. Zhang, G.S. Fu, *J. Appl. Phys.* **103**, 093901 (2008).
20. L. Zhao, J. Lian, Y. Liu, Q. Jiang. *Appl. Surf. Sci.* **252**, 8451 (2006).
21. S. Singh, M.S.R. Rao, *Phy. Rev. B* **80**, 045210 (2009).
22. B. Wu, Q.Y. Xu, F.M. Zhang, X.S. Liu, Y.W. Du, *AAPPS Bulletin* **18**, 52 (2008).